CMOS compatible source of single photons at near-visible wavelengths

ROBERT CERNANSKY[1], FRANCESCO MARTINI[1], AND ALBERTO POLITI[1,*]

[1] Department of Physics and Astronomy, University of Southampton, Southampton, SO17 1BJ, United Kingdom
[*] Corresponding author: A.Politi@soton.ac.uk

Compiled January 12, 2018

We demonstrate on chip generation of correlated pairs of photons in the near-visible spectrum using a CMOS compatible PECVD Silicon Nitride photonic device. Photons are generated via spontaneous four wave mixing enhanced by a ring resonator with high intrinsic quality Q-factor of 320,000 resulting in a generation rate of 950,000 $\frac{pairs}{mW}$. The high brightness of this source offers the opportunity to expand photonic quantum technologies over a broad wavelength range and provides a path to develop fully integrated quantum chips working at room temperature.

OCIS codes: (270.0270) Quantum Optics; (190.4390) Nonlinear optics, integrated optics.

http://dx.doi.org/10.1364/ao.XX.XXXXXX

Non-classical states of light generated through spontaneous four wave mixing (SFWM) has been an essential source for integrated quantum photonic structures [1–3]. Highly enhanced light-matter interactions can be achieved by microring resonators due to constructing interference yielding to an efficient production of time-bin entangled photons [4, 5] useful for quantum computation [6], simulation [7] and quantum key distribution [8]. The enhanced generation rate of single photons relies on high quality factor Q and small modal volume V of the resonator, therefore low losses and small rings are highly desirable. So far there has been an intensive investigation of on chip integrated sources generating photons at telecom wavelengths [9–11]. This focus has been highly motivated not only because of the advanced technologies in integrated silicon photonics [12] and low loss fabrication of silica waveguides, but also for the straightforward application in quantum cryptography systems due to a long history of classical communications via low loss optical fibres [13]. The downfall of working at telecom wavelengths resides in the use of high performance superconducting detectors working at cryogenic temperatures that limits the scalability and potential commercialization of these devices. Placing the sample in a cryostat also precludes the use of modulators based on the thermo-optical effects, commonly used in present silicon devices for quantum optics [9]. In order to avoid working in cryogenic temperatures, we investigated photon pair generation in the near visible region. The possible integration of silicon avalanche photodetectors would result in a fully integrated quantum photonic chip working at room temperature.

Silicon nitride (SiN) is a CMOS compatible material [14] with a high refractive index of 2 that exhibits moderate $\chi^{(3)}$ nonlinearity. It has been used both to generate single photons [15] as well as to manipulate quantum states [16, 17] at telecom wavelengths. Thanks to the high bandgap of $5eV$, SiN is the ideal candidate to design SFWM sources near the visible range and promises direct integration with silicon components. In this Letter we demonstrate generation rates of more than 2 million pairs of photons in the near visible range in a small ($19\mu m$ radius), low loss ($2.2dB/cm$) SiN ring resonator. The source developed here can find application in quantum networks, as the wavelengths and bandwidths are compatible with solid-state quantum memories [18], systems based on Raman schemes with hot atomic vapors [19] as well as free space communication channels [20].

In order to minimize the field overlap with the waveguide sidewall and optimize confinement and loss propagation, we designed devices with dimensions of $400x700nm$, showing multimode behavior. The fundamental TE mode used for this experiment is reported in (Fig. 1(a)). To couple light from SiN waveguides to optical fibers, we optimized apodized gratings following the algorithm described in reference [21]. In order to reduce lithography steps we designed the gratings to be fully etched, while apodization maintained a simulated coupling efficiency of 38% and a $3dB$ bandwidth of more than $20nm$, as shown in Fig. 1(b). Mode converters are used to reshape the optical mode adiabatically so that losses are minimized while changing the transverse size of the waveguide from $13\mu m$ to $700nm$ in a length of 350 μm.

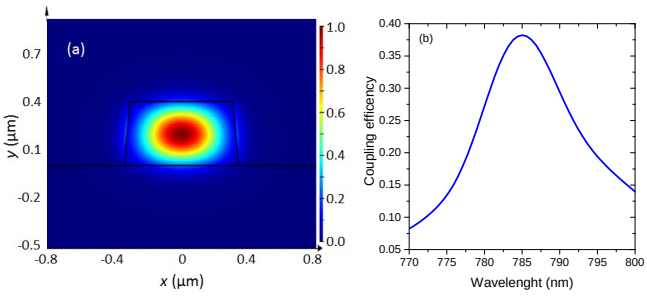

Fig. 1. (a) Fundamental TE mode of the SiN waveguide. (b) Coupling efficiency of apodized grating coupler.

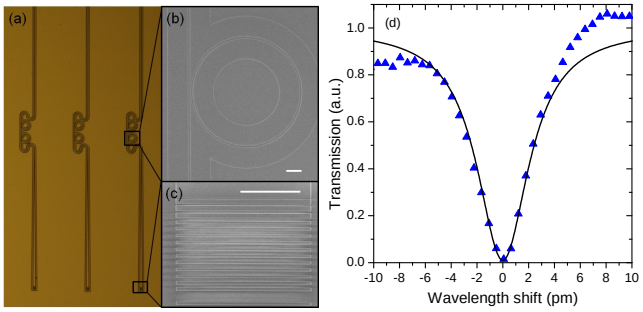

Fig. 2. (a) Optical picture of the fabricated photonic chip, with SEM pictures illustrating (b) the ring resonator and (c) apodized grating coupler (scale bars correspond to 5μm). (d) Transmission measurement of the ring resonator used for SFWM (triangles), and best fit (solid line) showing a close to critically coupled resonance with intrinsic Q-factor of 320.000 at a wavelength of 784.5 nm.

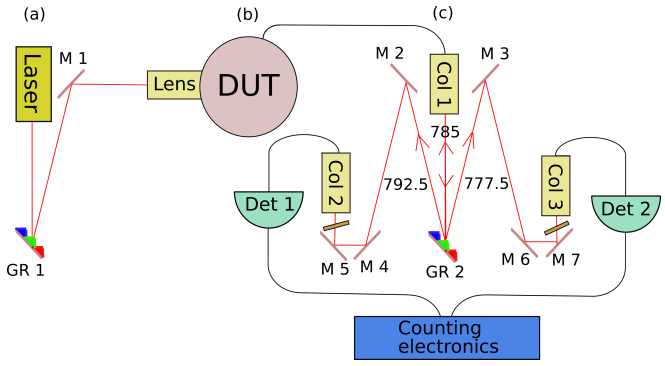

Fig. 3. Schematic setup for on chip generation and measurement of single photons. (a) Spectral filter of the noise generated from the pump laser. (b) Coupling to the SiN chip and generation of signal and idler photons. (c) Free-space optics to separate the generated photons and remove the pump stray light. GR: diffraction grating, M: mirror, Col: collimation optics.

The photonic devices were fabricated starting from 2μm of low loss thermal SiO_2 grown by wet oxidation on top of a standard silicon wafer. Then we deposited 410nm PECVD SiN with a 5:2 ratio of NH_3:SiH_4 to minimize the amount of silicon nanoclusters [22], showing a refractive index of 1.97 at 785nm and stress comparable with stoichiometric SiN. Samples were diced and spun with 450nm of CSAR, before being exposed with an electron beam lithography system JEOL JBX-9300FS. After the lithography step we developed the resist and etched the sample with ICP RIE. We removed the resist leftover and deposited 1.2μm of PECVD TEOS SiO_2 as top cladding. All the fabrication steps after the wet oxidation process were performed in temperatures not exceeding 350 degrees, making PECVD SiN compatible with Back End of Line CMOS processes. An optical image and SEM details of the photonic chip are reported in Fig. 2(a)-(c). Devices were optically characterized by performing transmission measurements with a DFB tunable laser (Thorlabs). We fabricate two rings resonators for every input waveguide, so that the resonance spacing (equal to half the FSR of 2.5 nm) is smaller than the tuning range of the laser (2nm). Fig. 2(d) displays the transmission of a critically coupled ring with 19μm radius with an intrinsic Q-factor of 320,000. From this value we can extract the propagation losses of the structure to be 2.2dB/cm. The measured coupling efficiency from fiber array to wavveguide corresponds to -11dB.

We designed an experimental setup to measure SFWM that consists of three parts (Fig. 3). The first part in Fig. 3(a) is composed by spectral filtering to reduce the laser sideband noise to the level of the single photons. This was achieved with one dispersive grating whose stray light reduction is 60dB at frequencies of signal (777nm) and idler (792nm). The filtered beam was then coupled via a high NA objective to the 2mm long input waveguide (coupling efficiency -4.8dB), shown in Fig. 3(b). We used free space coupling for the input to avoid any spurious light generated in optical fibers. The pump laser was coupled to the ring resonator under test where it was attenuated by 23dB due to the destructive interference of the resonator, and simultaneously the twin photons were generated. Signal, pump and idler photons were then coupled to a fiber array thanks to the grating coupler. The last part of the setup, Fig. 3(c), was used to separate the signal and idler photons and reject the pump light. In order to separate the correlated photons we used a dispersive grating in Littrow configuration where the pump wavelength is back reflected while the signal and idler are diffracted to opposite angles. Additional rejection was provided by 3 nm bandwidth filters centered at respective signal/idler wavelength. The single photons were finally coupled to single mode fibers and detected by silicon avalanche photodiode detectors with quantum efficiency of 65% (Excelitas). The electric signals were recorded by counting electronics and a time interval analyzer (Picoquant) to measure single and coincidence counts.

From the coincidence measurement we were able to extract the information about generated single photons in the ring coupled to the waveguide. The experimental data of generated pairs are extracted from the equation

$$G_{SFWM} = \frac{P^{SFWM}}{2\hbar\omega_p} = \frac{CC}{10^{-(\eta_s+\eta_i)/10}}, \quad \textbf{(1)}$$

where CC are measured coincidences, $\eta_{s/i}$ are the overall collection losses for the signal and idler, which in our case are 16.4dB and 24.1dB, respectively. P^{SFWM} is the power of measured photons based on the equation [23]

$$P^{SFWM} = (\gamma L)^2 \left(\frac{Q_l v_p}{\omega_p L/2}\right)^3 \frac{\hbar\omega_p v_p}{2L} P_p^2, \quad \textbf{(2)}$$

where γ is the nonlinear parameter, L is the circumference of the ring, P_p is power of the pump in the ring, Q_l is the measured loaded Q factor. The nonlinear parameter is defined in as the usual $\gamma = \frac{2\pi n_{nl}}{\lambda_p A_{eff}}$, where we used the nonlinear index $n_{nl} = 2.3 \cdot 10^{-19} m^2/W$ from literature [24]. The mode effective area $A_{eff} = 0.27\mu m^2$ and group velocity $v_p = c/2.04$ of the fundamental mode were numerically calculated. We can conclude that the experimental data in Fig. 4 are in a good agreement with the theoretical model of Eq. 1. This confirms the nonlinear relationship between the generated single photons and pump photons with a generation rate of $950,000 \frac{pairs}{mW}$.

Beside the photon pair generation rate, an important figure of merit to characterize the quality of a correlated photon pair source is the coincidence CC to accidental AC ratio CAR. It takes into account the relationship between the number of SFWM photon pairs and the number of accidental coincidences, coming

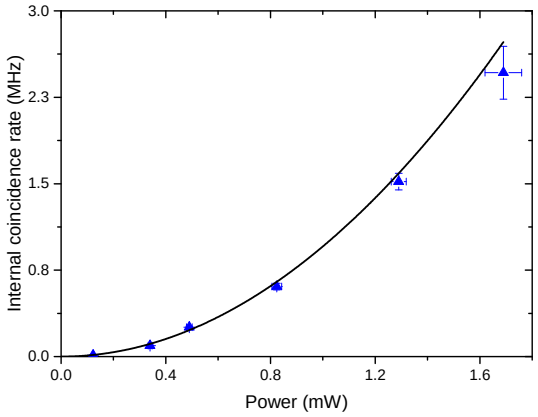

Fig. 4. Measured (triangles) and theoretical (solid line) internal coincidence rate at the ring location as a function of the power coupled into the chip. The rate is estimated considering the measured rates with 1152ps time integration and accounting for system losses

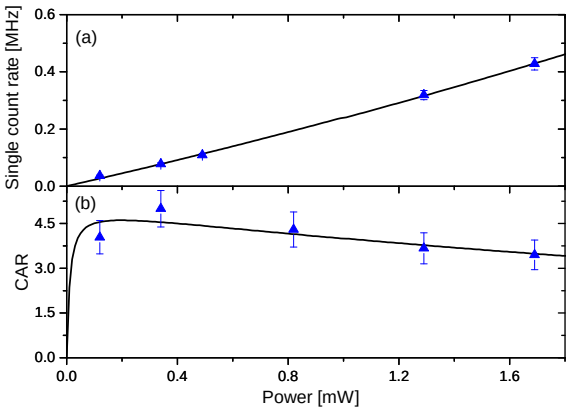

Fig. 5. (a) Measured (triangles) and theoretical (solid line) power dependence of the single photon generation at the signal wavelength (777.5nm) fitted by linear function. (b) Measured (triangles) and theoretical (solid line) power dependence of the Coincidence to Accidental Ratio (CAR).

from photons emitted randomly in time

$$CAR = \frac{CC}{AC}, \tag{3}$$

$$CC = G_{SFWM}\eta_s\eta_i, \tag{4}$$

$$AC = R_sR_i\delta t, \tag{5}$$

$$R_s = (n_s + G_{SFWM})\,\eta_s + dc_s, \tag{6}$$

$$R_i = (n_i + G_{SFWM})\,\eta_i + dc_i, \tag{7}$$

where CAR depends on the integration time δt and dark counts of the detectors $dc_{s/i}$, and any linear noise $n_{s/i}$ resulting from the light interaction in the material. $R_{s/i}$ are the measured singles at signal and idler frequency, respectively. In Fig. 5(a) we report the power dependence of the detected signal photons R_s, showing a linear dependence. We confirmed these photons are generated in the ring by comparing to off-resonance pumping. The linear relation suggests that the ring resonator emits uncorrelated photons generated from spontaneous Raman scattering, as suggested by the broad scattering spectrum of SiN [25].

In Fig. 5(b) we characterized the CAR as a function of the power in the waveguide. The number of coincidences and accidental counts is measured with a time window of 1152 ps, longer than the FWHM value of the coincidence peak of $\sim 500ps$. This is to ensure that all the coincidence counts are included, at the expense of a lower CAR [26]. Moreover, the FWHM value is mainly dictated by the jitter of our Si detectors, rather than the lifetime of the photons ($< 200ps$, considering the Q factor of our cavity). Faster detectors, or pulsed excitation, would result in a higher measured CAR. Fig. 5(b) also includes a curve from equations 3-7 where the parameters are extracted from Fig. 4, considering correction of signal and idler photons by respective phonon distribution [27], and 5(a) without fitting any additional variable. The model shows good agreement with data, indicating that the CAR value is limited from Raman photons at all the powers used in the experiment. Effects from detector dark counts are only visible at very low pump powers, while multi-photon events cause a small decrease in CAR for increasing power in the tested range. These results are comparable to CAR measurements in strip SiN waveguides [28] and Hydex rings resonators [29] at telecom wavelengths, once the detection timing is considered.

In conclusion, we studied spontaneous four wave mixing process in the near visible region generated in a microring resonator. Contrary to alternative sources based on periodically pooled crystals [30, 31] the CMOS compatible fabrication process would make possible the integration of non-classical sources together with silicon based detectors working at room temperature. We believe that the measured CAR is mainly limited by the linear noise coming from uncorrelated Raman photons which affects amorphous materials, including Silicon Nitride. Optimization of the optical properties of SiN through tailored material deposition, combined with the design parameters for the ring resonator, can lead to an increase of generation rate and CAR value. Moreover, an increase of Q factor will reduce the bandwidth of the generated photons from the current 2.4GHz to sub-GHz values, optimising the coupling efficiency of the source to atomic memories. Finally, the confirmed absence of saturation in the pair generation rate, thanks to the high bandgap of SiN, suggests that integrated single photon sources can be developed well in the visible spectrum. These properties make SiN resonators excellent candidates to expand the applications of integrated single photon sources for a broad range of quantum technology applications.

FUNDING INFORMATION

This work was supported by the H2020-FETPROACT-2014 Grant QUCHIP (Quantum Simulation on a Photonic Chip; grant agreement no. 641039).

ACKNOWLEDGMENTS

We acknowledge support from the Southampton Nanofabrication Centre.

REFERENCES

1. J. E. Sharping, K. F. Lee, M. a. Foster, A. C. Turner, B. S. Schmidt, M. Lipson, A. L. Gaeta, and P. Kumar, Optics express **14**, 12388 (2006).
2. H. Takesue, Y. Tokura, H. Fukuda, T. Tsuchizawa, T. Watanabe, K. Yamada, and S.-i. Itabashi, Applied Physics Letters **91**, 201108 (2007).

3. S. Clemmen, K. Phan Huy, W. Bogaerts, R. G. Baets, P. Emplit, and S. Massar, Optics express **17**, 16558 (2009).
4. S. Azzini, D. Grassani, M. J. Strain, M. Sorel, L. G. Helt, J. E. Sipe, M. Liscidini, M. Galli, and D. Bajoni, Opt. Express **20**, 23100 (2012).
5. D. Grassani, S. Azzini, M. Liscidini, M. Galli, M. J. Strain, M. Sorel, J. E. Sipe, and D. Bajoni, Optica **2**, 88 (2015).
6. E. Knill, R. Laflamme, and G. J. Milburn, Nature **409**, 46 (2001).
7. A. Aspuru-Guzik and P. Walther, Nature Physics **8**, 285 (2012).
8. N. Gisin and R. Thew, Nature Photonics **1**, 165 (2007).
9. J. W. Silverstone, D. Bonneau, K. Ohira, N. Suzuki, H. Yoshida, N. Iizuka, M. Ezaki, C. M. Natarajan, M. G. Tanner, R. H. Hadfield, V. Zwiller, G. D. Marshall, J. G. Rarity, J. L. O'Brien, and M. G. Thompson, Nature Photonics **8**, 104 (2013).
10. H. Jin, F. M. Liu, P. Xu, J. L. Xia, M. L. Zhong, Y. Yuan, J. W. Zhou, Y. X. Gong, W. Wang, and S. N. Zhu, Physical Review Letters **113**, 103601 (2014).
11. S. F. Preble, M. L. Fanto, J. a. Steidle, C. C. Tison, G. a. Howland, Z. Wang, and P. M. Alsing, Physical Review Applied **4**, 021001 (2015).
12. C. Xiong, B. Bell, and B. J. Eggleton, Nanophotonics **5**, 22 (2016).
13. S. Ten, "Ultra low-loss optical fiber technology," in "2016 Optical Fiber Communications Conference and Exhibition (OFC)," (2016), pp. 1–3.
14. D. J. Moss, R. Morandotti, A. L. Gaeta, and M. Lipson, Nature Photonics **7**, 597 (2013).
15. S. Ramelow, A. Farsi, S. Clemmen, D. Orquiza, K. Luke, M. Lipson, and A. L. Gaeta p. 1508.04358 (2015).
16. C. Xiong, X. Zhang, A. Mahendra, J. He, D.-Y. Choi, C. J. Chae, D. Marpaung, A. Leinse, R. G. Heideman, M. Hoekman, C. G. H. Roeloffzen, R. M. Oldenbeuving, P. W. L. van Dijk, C. Taddei, P. H. W. Leong, and B. J. Eggleton, Optica **2**, 724 (2015).
17. A. Mohanty, M. Zhang, A. Dutt, S. Ramelow, P. Nussenzveig, and M. Lipson, Nature Communications **8**, 14010 (2017).
18. E. Saglamyurek, N. Sinclair, J. Jin, J. A. Slater, D. Oblak, F. Bussières, M. George, R. Ricken, W. Sohler, and W. Tittel, Nature **469**, 512 (2011).
19. K. F. Reim, J. Nunn, V. O. Lorenz, B. J. Sussman, K. C. Lee, N. K. Langford, D. Jaksch, and I. A. Walmsley, Nature Photonics **4**, 218 (2010).
20. J. Yin, Y. Cao, Y.-H. Li, S.-K. Liao, L. Zhang, J.-G. Ren, W.-Q. Cai, W.-Y. Liu, B. Li, H. Dai, G.-B. Li, Q.-M. Lu, Y.-H. Gong, Y. Xu, S.-L. Li, F.-Z. Li, Y.-Y. Yin, Z.-Q. Jiang, M. Li, J.-J. Jia, G. Ren, D. He, Y.-L. Zhou, X.-X. Zhang, N. Wang, X. Chang, Z.-C. Zhu, N.-L. Liu, Y.-A. Chen, C.-Y. Lu, R. Shu, C.-Z. Peng, J.-Y. Wang, and J.-W. Pan, Science **356**, 1140 (2017).
21. F. Martini and A. Politi, Optics Express **25**, 10735 (2017).
22. A. Gorin, A. Jaouad, E. Grondin, V. Aimez, and P. Charette, Optics Express **16**, 13509 (2008).
23. L. G. Helt, M. Liscidini, and J. E. Sipe, J. Opt. Soc. Am. B **29**, 2199 (2012).
24. C. Lacava, S. Stankovic, A. Z. Khokhar, T. D. Bucio, F. Y. Gardes, G. T. Reed, D. J. Richardson, and P. Petropoulos, Scientific Reports **7**, 22 (2017).
25. A. Dhakal, P. Wuytens, A. Raza, N. Le Thomas, and R. Baets, Materials **10** (2017).
26. E. Engin, D. Bonneau, C. M. Natarajan, A. S. Clark, M. G. Tanner, R. H. Hadfield, S. N. Dorenbos, V. Zwiller, K. Ohira, N. Suzuki, H. Yoshida, N. Iizuka, M. Ezaki, J. L. O'Brien, and M. G. Thompson, Optics express **21**, 27826 (2013).
27. H. Takesue and K. Inoue, Opt. Express **13**, 7832 (2005).
28. X. Zhang, Y. Zhang, C. Xiong, and B. J. Eggleton, Journal of Optics **18**, 074016 (2016).
29. C. Reimer, L. Caspani, M. Clerici, M. Ferrera, M. Kues, M. Peccianti, A. Pasquazi, L. Razzari, B. E. Little, S. T. Chu, D. J. Moss, and R. Morandotti, Opt. Express **22**, 6535 (2014).
30. K. Sanaka, K. Kawahara, and T. Kuga, Phys. Rev. Lett. **86**, 5620 (2001).
31. K. Banaszek, A. B. U'Ren, and I. A. Walmsley, Opt. Lett. **26**, 1367 (2001).

FULL REFERENCES

1. J. E. Sharping, K. F. Lee, M. a. Foster, A. C. Turner, B. S. Schmidt, M. Lipson, A. L. Gaeta, and P. Kumar, "Generation of correlated photons in nanoscale silicon waveguides." Optics express **14**, 12388–93 (2006).
2. H. Takesue, Y. Tokura, H. Fukuda, T. Tsuchizawa, T. Watanabe, K. Yamada, and S.-i. Itabashi, "Entanglement generation using silicon wire waveguide," Applied Physics Letters **91**, 201108 (2007).
3. S. Clemmen, K. Phan Huy, W. Bogaerts, R. G. Baets, P. Emplit, and S. Massar, "Continuous wave photon pair generation in silicon-on-insulator waveguides and ring resonators." Optics express **17**, 16558–70 (2009).
4. S. Azzini, D. Grassani, M. J. Strain, M. Sorel, L. G. Helt, J. E. Sipe, M. Liscidini, M. Galli, and D. Bajoni, "Ultra-low power generation of twin photons in a compact silicon ring resonator," Opt. Express **20**, 23100–23107 (2012).
5. D. Grassani, S. Azzini, M. Liscidini, M. Galli, M. J. Strain, M. Sorel, J. E. Sipe, and D. Bajoni, "Micrometer-scale integrated silicon source of time-energy entangled photons," Optica **2**, 88 (2015).
6. E. Knill, R. Laflamme, and G. J. Milburn, "A scheme for efficient quantum computation with linear optics." Nature **409**, 46–52 (2001).
7. A. Aspuru-Guzik and P. Walther, "Photonic quantum simulators," Nature Physics **8**, 285–291 (2012).
8. N. Gisin and R. Thew, "Quantum communication," Nature Photonics **1**, 165–171 (2007).
9. J. W. Silverstone, D. Bonneau, K. Ohira, N. Suzuki, H. Yoshida, N. Iizuka, M. Ezaki, C. M. Natarajan, M. G. Tanner, R. H. Hadfield, V. Zwiller, G. D. Marshall, J. G. Rarity, J. L. O'Brien, and M. G. Thompson, "On-chip quantum interference between silicon photon-pair sources," Nature Photonics **8**, 104–108 (2013).
10. H. Jin, F. M. Liu, P. Xu, J. L. Xia, M. L. Zhong, Y. Yuan, J. W. Zhou, Y. X. Gong, W. Wang, and S. N. Zhu, "On-Chip Generation and Manipulation of Entangled Photons Based on Reconfigurable Lithium-Niobate Waveguide Circuits," Physical Review Letters **113**, 103601 (2014).
11. S. F. Preble, M. L. Fanto, J. a. Steidle, C. C. Tison, G. a. Howland, Z. Wang, and P. M. Alsing, "On-Chip Quantum Interference from a Single Silicon Ring-Resonator Source," Physical Review Applied **4**, 021001 (2015).
12. C. Xiong, B. Bell, and B. J. Eggleton, "CMOS-compatible photonic devices for single-photon generation," Nanophotonics **5**, 22 (2016).
13. S. Ten, "Ultra low-loss optical fiber technology," in "2016 Optical Fiber Communications Conference and Exhibition (OFC)," (2016), pp. 1–3.
14. D. J. Moss, R. Morandotti, A. L. Gaeta, and M. Lipson, "New CMOS-compatible platforms based on silicon nitride and Hydex for nonlinear optics," Nature Photonics **7**, 597–607 (2013).
15. S. Ramelow, A. Farsi, S. Clemmen, D. Orquiza, K. Luke, M. Lipson, and A. L. Gaeta, "Silicon-Nitride Platform for Narrowband Entangled Photon Generation," p. 1508.04358 (2015).
16. C. Xiong, X. Zhang, A. Mahendra, J. He, D.-Y. Choi, C. J. Chae, D. Marpaung, A. Leinse, R. G. Heideman, M. Hoekman, C. G. H. Roeloffzen, R. M. Oldenbeuving, P. W. L. van Dijk, C. Taddei, P. H. W. Leong, and B. J. Eggleton, "Compact and reconfigurable silicon nitride time-bin entanglement circuit," Optica **2**, 724 (2015).
17. A. Mohanty, M. Zhang, A. Dutt, S. Ramelow, P. Nussenzveig, and M. Lipson, "Quantum interference between transverse spatial waveguide modes," Nature Communications **8**, 14010 (2017).
18. E. Saglamyurek, N. Sinclair, J. Jin, J. A. Slater, D. Oblak, F. Bussières, M. George, R. Ricken, W. Sohler, and W. Tittel, "Broadband waveguide quantum memory for entangled photons," Nature **469**, 512–5 (2011).
19. K. F. Reim, J. Nunn, V. O. Lorenz, B. J. Sussman, K. C. Lee, N. K. Langford, D. Jaksch, and I. A. Walmsley, "Towards high-speed optical quantum memories," Nature Photonics **4**, 218–221 (2010).
20. J. Yin, Y. Cao, Y.-H. Li, S.-K. Liao, L. Zhang, J.-G. Ren, W.-Q. Cai, W.-Y. Liu, B. Li, H. Dai, G.-B. Li, Q.-M. Lu, Y.-H. Gong, Y. Xu, S.-L. Li, F.-Z. Li, Y.-Y. Yin, Z.-Q. Jiang, M. Li, J.-J. Jia, G. Ren, D. He, Y.-L. Zhou, X.-X. Zhang, N. Wang, X. Chang, Z.-C. Zhu, N.-L. Liu, Y.-A. Chen, C.-Y. Lu, R. Shu, C.-Z. Peng, J.-Y. Wang, and J.-W. Pan, "Satellite-based entanglement distribution over 1200 kilometers," Science **356**, 1140–1144 (2017).
21. F. Martini and A. Politi, "Linear integrated optics in 3C silicon carbide," Optics Express **25**, 10735 (2017).
22. A. Gorin, A. Jaouad, E. Grondin, V. Aimez, and P. Charette, "Fabrication of silicon nitride waveguides for visible-light using PECVD: a study of the effect of plasma frequency on optical properties," Optics Express **16**, 13509 (2008).
23. L. G. Helt, M. Liscidini, and J. E. Sipe, "How does it scale? comparing quantum and classical nonlinear optical processes in integrated devices," J. Opt. Soc. Am. B **29**, 2199–2212 (2012).
24. C. Lacava, S. Stankovic, A. Z. Khokhar, T. D. Bucio, F. Y. Gardes, G. T. Reed, D. J. Richardson, and P. Petropoulos, "Si-rich Silicon Nitride for Nonlinear Signal Processing Applications," Scientific Reports **7**, 22 (2017).
25. A. Dhakal, P. Wuytens, A. Raza, N. Le Thomas, and R. Baets, "Silicon nitride background in nanophotonic waveguide enhanced raman spectroscopy," Materials **10** (2017).
26. E. Engin, D. Bonneau, C. M. Natarajan, A. S. Clark, M. G. Tanner, R. H. Hadfield, S. N. Dorenbos, V. Zwiller, K. Ohira, N. Suzuki, H. Yoshida, N. Iizuka, M. Ezaki, J. L. O'Brien, and M. G. Thompson, "Photon pair generation in a silicon micro-ring resonator with reverse bias enhancement." Optics express **21**, 27826–34 (2013).
27. H. Takesue and K. Inoue, "1.5-μm band quantum-correlated photon pair generation in dispersion-shifted fiber: suppression of noise photons by cooling fiber," Opt. Express **13**, 7832–7839 (2005).
28. X. Zhang, Y. Zhang, C. Xiong, and B. J. Eggleton, "Correlated photon pair generation in low-loss double-stripe silicon nitride waveguides," Journal of Optics **18**, 074016 (2016).
29. C. Reimer, L. Caspani, M. Clerici, M. Ferrera, M. Kues, M. Peccianti, A. Pasquazi, L. Razzari, B. E. Little, S. T. Chu, D. J. Moss, and R. Morandotti, "Integrated frequency comb source of heralded single photons," Opt. Express **22**, 6535–6546 (2014).
30. K. Sanaka, K. Kawahara, and T. Kuga, "New high-efficiency source of photon pairs for engineering quantum entanglement," Phys. Rev. Lett. **86**, 5620–5623 (2001).
31. K. Banaszek, A. B. U'Ren, and I. A. Walmsley, "Generation of correlated photons in controlled spatial modes by downconversion in nonlinear waveguides," Opt. Lett. **26**, 1367–1369 (2001).